

A critical evaluation of PCA detection of polarized signatures using real stellar data

Frédéric Paletou

¹ Université de Toulouse, UPS-Observatoire Midi-Pyrénées, Irap, Toulouse, France

² CNRS, Institut de Recherche en Astrophysique et Planétologie, 14 av. E. Belin, 31400 Toulouse, France
e-mail: fpaletou@irap.omp.eu

Received April 12, 2012; accepted June 22, 2012

ABSTRACT

The general context of this study concerns the post-processing of multiline spectropolarimetric observations of stars, and in particular these numerical analysis techniques aiming at the detection and the characterization of polarized signatures. Hereafter, using real observational data, we compare and clarify a number of points concerning various methods of analysis. Indeed, simple line addition, least-squares deconvolution and denoising by principal component analysis have been applied, and compared to each other, to polarized stellar spectra available from the TBLegacy database of the Narval spectropolarimeter. Such a comparison between various approaches of distinct sophistication levels allows us to make a safe choice for the next implementation of on-line post-processing of our unique database for the stellar physics community.

Key words. Methods: data analysis – Polarization – Stars: magnetic fields – Astronomical databases: miscellaneous

1. Introduction

The present study concerns the post-processing of multiline spectropolarimetric measurements, and in particular of stellar data. We focus hereafter on data collected, since 2006, with the Narval spectropolarimeter mounted at the 2-m aperture TBL telescope located at the summit of the *Pic du Midi de Bigorre* (France). We investigate, in particular, the capabilities of principal component analysis (hereafter PCA) on observations made with Narval.

PCA has been regularly used in *solar* spectropolarimetry during the last decade (see e.g., Rees et al. 2000 and Skumanich & López Ariste 2002). Its main purpose was to provide an alternative way of inverting spectropolarimetric data, for the determination of the vector magnetic field present in various solar features, from sunspots to solar prominences (see e.g., López Ariste & Casini 2002).

Concerning stellar data, PCA-based denoising of spectral lines was first presented by Carroll et al. (2007). It was further tested on data taken with the SOFIN spectrograph at the NOT telescope. This procedure was mainly driven by the purpose of doing Zeeman-Doppler Imaging (hereafter ZDI; see Semel 1989) from temporal sequences of individual spectral lines, instead of using pseudo-profiles such as the ones commonly computed by least-squares deconvolution (hereafter LSD; see Donati et al. 1997 and Kochukhov et al. 2010, for a recent review and discussion). More recently, Martínez González et al. (2008) discussed in details the capabilities of PCA denoising of solar and stellar spectropolarimetric data, using *synthetic* data. They also provided some comments concerning the relationship between PCA denoising, line addition and least-squares deconvolution. Later on, Ramírez Vélez et al. (2010) proposed another PCA-based method, coupled to ZDI, which was applied to a very limited set of observational data taken both at the AAT telescope

with the SemelPol spectropolarimeter, and with Narval at the TBL.

Hereafter we come back on some details of PCA denoising and analysis of *observational* spectropolarimetric data. We discuss further the practical capabilities of such an approach. Comparisons with LSD and the so-called (simple) line addition (hereafter SLA; Semel et al. 2009) methods are also discussed.

2. The source of data

We have been using Narval data available from the *public* database TBLegacy¹. Narval is a state-of-the-art spectropolarimeter operating in the 0.38-1 μm spectral domain, with a spectral resolution of 65 000 in its polarimetric mode. It is an improved copy, adapted to the 2-m TBL telescope, of the Espadons spectropolarimeter, in operations since 2004 at the 3.6-m aperture CFHT telescope (see Donati et al. 2006 for further technical details).

The TBLegacy database is operational since 2007. It is at the present time the largest on-line archive of high-resolution polarization spectra. It hosts data which were taken at the 2-m TBL telescope since december 2006. So far, more than 70 000 spectra have been made available, for more than 370 distinct targets all over the Hertzsprung-Russell diagram. More than 13 000 *polarized* spectra are also available, mostly for *circular* polarization (linear polarization data are very seldom still and amounts to a few hundreds spectra, but it is equally available). By default, the latter is the usual circular polarization $V(\lambda)/I_c$ normalized to the local continuum intensity.

At the present time, the TBLegacy database provides no more than Stokes I or V/I_c spectra calibrated in wavelength. Stokes I data are either normalised to the local continuum or not.

¹ <http://tblegacy.bagn.obs-mip.fr/>

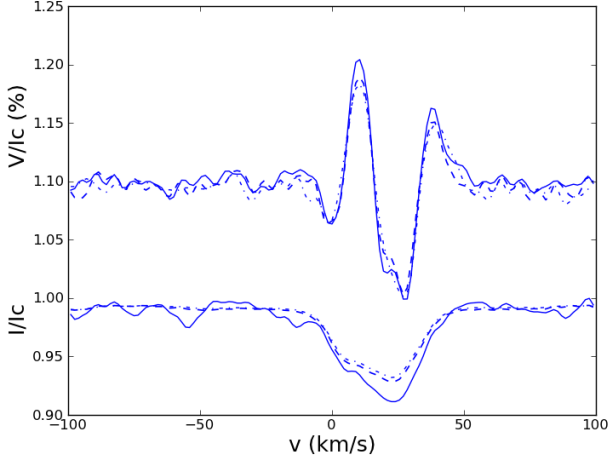


Fig. 1. Comparison between LSD (full lines) and SLA (dashed lines) I/I_c and V/I_c pseudo-line profiles, for II Peg observations of August 2008. Stokes V profiles have been shifted by 1.1 so the largest amplitude lobe, for LSD, is about 0.1% of I_c in that case. P_1 profiles (dot-dashed) both for I/I_c and V/I_c resulting from PCA analysis of the data are also displayed for comparison purpose.

In a next step, further post-processing of these spectra will be proposed on-line to users and the relevant software will be made fully available to the community. It will be the case for the simple line addition and the least-squares deconvolution standard procedures that we shall be using in the present study, together with PCA denoising.

3. Numerical procedures

3.1. The matrix of observations

Observations we get from TBLegacy are basically Stokes $I(\lambda)$ or $V(\lambda)$. Each of them consist in a very large array of about 200 000 elements covering the whole spectral domain observable by Narval. The main task of building the matrix of observations \mathbf{O} is to split the multiline observations vs. wavelength into N_{obs} elementary profiles, each of them centered at a given wavelength and projected onto a common *velocity* grid. Such a velocity grid is an *a priori* data that we adopt in our numerical procedure. The choice of such a grid of velocities depends on the spectral sampling of the original set of data – in the case of Narval data it is of the order of 1.8 km.s^{-1} , as well as on the target nature, for what concerns the velocity range to be considered (typically between ± 120 and $\pm 200 \text{ km.s}^{-1}$). Practically we shall be dealing with N_v velocity bins of the order of 10^2 , while I or V original data (sampled in wavelength), will be recast into N_{obs} elementary v -sampled profiles, where N_{obs} is of the order of 10^3 - 10^4 , depending on the spectral type of the target.

The transformation of the original data requires the help of a supplementary file, usually called “mask” and which consists in the list of all the wavelengths at rest, λ_0 , of the spectral lines expected to be present in the observations of a given spectral type of stars. For all of the cases discussed hereafter, we have used mask files widely used by the community and built from the VALD database (Piskunov et al. 1995; ressources for this study have been kindly provided to us by E. Alecian). In general, these mask files contain additional information about each

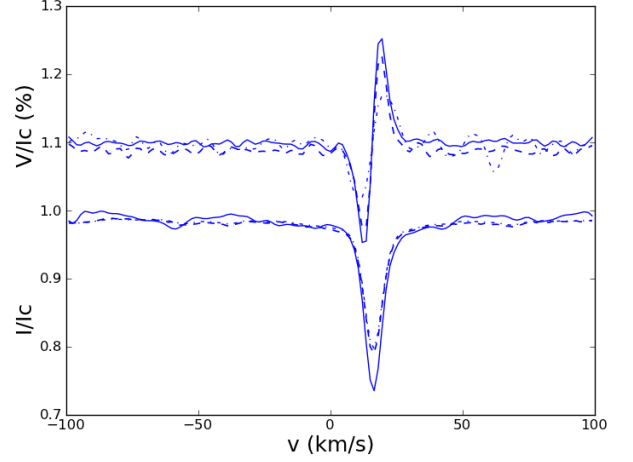


Fig. 2. Same as Fig. (1) but for ε Eri observations of February 2007. Stokes V profiles have been shifted by 1.1 and multiplied by 3, so the largest amplitude lobe, for LSD, is about 0.05% of I_c in that case.

spectral line, in particular their line depression, d_i , and effective Landé factors, g_i , required by LSD (see next section).

Therefore, given a proper mask and a velocity grid, it is quite easy and straightforward to transform $I(\lambda)$ or $V(\lambda)$ data into N_{obs} individual $I(v)$ or $V(v)$ profiles, in accordance with the Doppler-Fizeau effect and the well-known relationship

$$\frac{\delta v}{c} = \frac{\delta \lambda}{\lambda_0}, \quad (1)$$

where $\delta \lambda = (\lambda - \lambda_0)$, which is computed from the original data (see also §2.1 in Ramírez Vélez et al. 2010).

This operation results into the construction of a (N_{obs}, N_v) rectangular matrix of observations \mathbf{O} which shall now be used in different ways.

3.2. Simple line addition vs. LSD

For a wealth of data in TBLegacy, down to polarized signatures V/I_c of the order of 0.01%, the pseudo-profiles resulting from the simple line addition (or, to be more precise the *unweighted*, or arithmetic mean) of the N_{obs} individual spectral lines of \mathbf{O} are very meaningful, both from the standpoints of the detection and of the characterization (i.e., the proper determination of its shape and amplitudes) of the polarized signature carried by the multiline, but noisy, observations. Moreover, SLA profiles are very similar to the one obtained from least-squares deconvolution. This was indeed mentioned and discussed in the very instructive, but unfortunately overlooked at, recent article of Semel et al. (2009). Nevertheless, to the best of our knowledge, *no direct comparisons between LSD and SLA profiles obtained with real data such as Narval’s, have been published yet.*

To remedy that, in Figs. (1) and (2), we display both LSD and SLA pseudo-profiles obtained directly by computing a *simple average* of all the rows of the \mathbf{O} matrix constructed from the same set of observations of the RS CVn star II Peg, made in August 2008. The LSD profiles for Stokes I have been computed using weights $\omega_I = d_i$ normalized to the arithmetic mean of the considered central line depressions d_i . Those for Stokes V were computed for weights $\omega_V = g_i \lambda_{0,i} d_i$ normalized to the arithmetic mean of the ω_V ’s. Also, *no* line depth cut-off criterium

was adopted there (provided that depressions are, originally, greater than or equal to 10% of the continuum). Considerations and recommendations about the issue of LSD weights definition (and especially their normalisation) and line depth cut-off criterium can be found in Kochukhov et al. (2010). The latter revealed some indiscipline in the community of LSD users and subsequent articles still fail, unfortunately, in providing details about the exact procedure which was applied to data – see e.g., Kochukhov et al. (2011) or Donati et al. (2011). To conclude on these points, we again recommend this community to read carefully Semel et al. (2009) and, especially, their §2.3 dedicated to the statistical properties of (LSD) weights.

For II Peg, we considered about 6600 wavelengths in the mask, covering a 400-1000 nm range, using VALD data for a $T_{\text{eff.}} = 5000$ K, a surface gravity of $\log g = 3.0$ cgs and solar abundances. Concerning this choice of stellar parameters, Berdyugina et al. (1998) determined $T_{\text{eff.}} = 4600$ K and $\log g = 3.2$ cgs. However $T_{\text{eff.}}$ as high as 5250 K are still reported by VizieR. As can be seen in Fig. (1), respective shapes of I/I_c and V/I_c are well recovered, both by LSD and SLA, and they are indeed very similar. Amplitudes of I/I_c and V/I_c LSD pseudo-profiles appear systematically slightly larger than SLA ones. However, this is not going to impair significantly any further determination of the mean line-of-sight magnetic field usually made, assuming the weak-field regime of the Zeeman effect, using the centre of gravity method (Rees & Semel 1979, and references therein).

We noticed similar effects, displayed in Fig. (2), using observations of the K2V star ε Eri made on February 2007 with Narval. For that case, and after inspection of all VizieR ressources, we adopted a $T_{\text{eff.}} = 5000$ K and a surface gravity of $\log g = 4.5$ cgs (and solar abundances) mask (see also Koleva & Vazdekis 2012).

Using a test version of TBLegacy currently under development², we have been able to verify indeed how similar SLA and LSD signatures are, from the analysis of many other cases including for hotter magnetic stars than the ones discussed in this article.

3.3. Principal component analysis

Following Martínez González et al. (2008), we built the cross-product matrix, $\mathbf{C} = \mathbf{O}^T \mathbf{O}$, and computed its eigenvalues s_i and eigenvectors \mathbf{e}_i (hereafter, eigenprofiles). Hereafter we shall call $\mathbf{O}_j(v)$ the observation made at wavelength index j , and we shall omit the dependance in v of each of these individual profiles. No physical assumption about the line formation process or the origin of the polarization signals are required for the PCA analysis we have carried-out.

As demonstrated by Martínez González et al. (2008) with their Figs. (1), without any noise (or a limited amount of it – this is the case for Stokes I data from TBLegacy, for instance), the examination of the sequence of eigenvalues s_i of \mathbf{C} shows that a few of them will dominate, sometimes by orders of magnitudes as compared to the smallest ones. However, for significant noise levels, as it will be the case hereafter for Stokes V data, the sequence of s_i is in general very slowly decreasing - see e.g., Fig. (6).

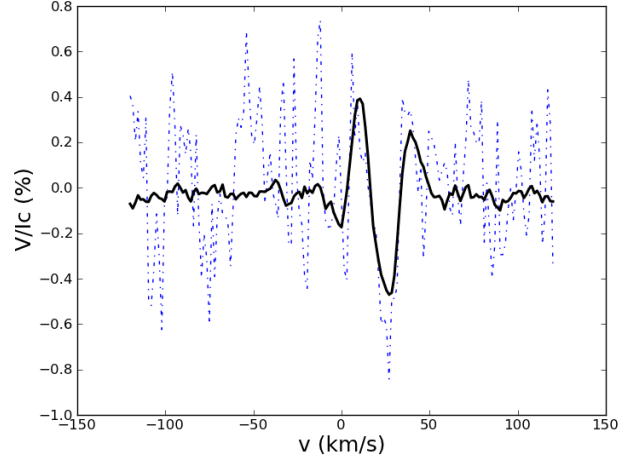


Fig. 3. Example of PCA denoising: the original noisy signal $\mathbf{O}_j(v)$ (dashed line) for the 612.2 nm line of Ca I, is displayed, together with its projection on the eigenprofile of matrix \mathbf{C} associated with the largest eigenvalue, $\mathbf{P}_{j,1}$ (full thick line). The latter profile already bears a shape very similar to the SLA (or LSD) pseudo-profiles obtained with the *whole* set of observations, and displayed in Fig. (1).

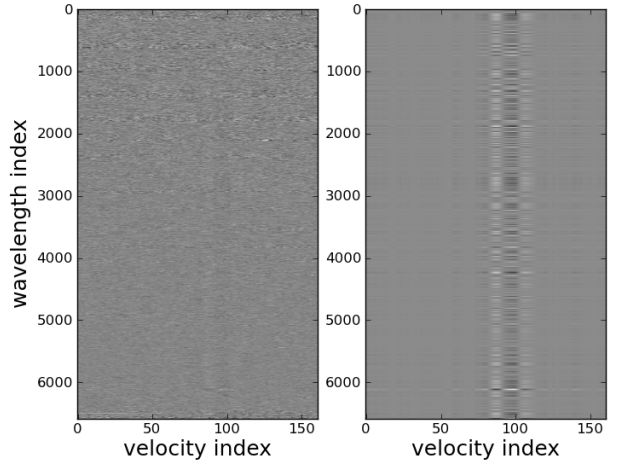


Fig. 4. Comparison between the original map of the matrix of observations \mathbf{O} (left) and the map of the $\mathbf{P}_{j,1}$ (right), for II Peg observations of August 2008. The efficiency of the PCA denoising is obvious at almost all wavelengths.

Even though the sequence of eigenvalues s_i is very slowly decreasing for most of Stokes V data from TBLegacy, we first tried PCA denoising by computing

$$\mathbf{P}_{j,k} = (\mathbf{O}_j \cdot \mathbf{e}_k) \mathbf{e}_k \quad (2)$$

for $k=1$. For the wavelength index j corresponding to the strong magnetically sensitive 612.2 nm line of Ca I, Fig. (3) shows the efficiency of PCA denoising using only the projection onto the eigenprofile \mathbf{e}_1 associated to the largest eigenvalue s_1 . In that case, it is quite obvious that, for that level of signal-to-noise ratio the gain provided by the PCA denoising procedure is significant enough, and potentially allows for the *detection* of a meaningful polarized signature buried into noise. Moreover, it

² The (Python) software implemented for such an analysis will be made public, although it is already available upon request to the author.

is easy to notice that the single $P_{j,1}$ denoised profile displayed in Fig. (3) already bears a shape very similar to the SLA (or LSD) pseudo-profiles obtained from *the whole set* of observations, as displayed in Fig. (1).

The efficiency of PCA denoising *at all wavelengths* can also be seen in Fig. (4) where we displayed images of the observations matrix \mathbf{O} (left) in comparison with the matrix of the $P_{j,1}$'s (right). In that case, clear polarized signatures emerge almost at all observed wavelengths. It also opens the possibility of a direct exploitation of single line data, instead of a pseudo-profile combining all of the multiline signatures. The same is true for ε Eri data, for instance, even though its SLA (or LSD) signature is significantly smaller than II Peg's.

4. Comparison with SLA and LSD

We have shown with the previous examples how PCA denoising can be efficient on real stellar data. It can be very useful for *detection* purpose but *could it offer an alternative to LSD or SLA methods?*

The case of ε Eri is interesting in the sense that its polarization signature is less complex but of much less amplitude than the one of II Peg. Both LSD and SLA pseudo-line profiles, that is:

$$\bar{O} = \frac{1}{N_{\text{obs}}} \sum_{j=1}^{N_{\text{obs}}} \mathbf{O}_j(v) \quad (3)$$

show a clear antisymmetric V/I_c profile with amplitudes of both negative and positive lobe about 0.04-0.05%, and spanning over a $\Delta v \approx 30 \text{ km.s}^{-1}$ spectral range. But this signature, recovered with two distinct methods, is not fully recovered when we consider just the mean of the projection of the \mathbf{O}_j 's onto eigenprofile e_1 only. The resulting mean profile is still about a factor of 2 less the amplitude of \bar{O} and the lobes are also wider than the ones of LSD or SLA pseudo-profiles – see again Fig. (2). Beyond the detection capability of PCA-based denoising, this opens the further question of the proper characterization of the “most common” polarization signal content of the multiline observations.

In order to investigate on that point, we built a map displayed in Fig. (5), constructed from the successive differences between

$$P_k = \frac{\sum_{j=1}^{N_{\text{obs}}} \sum_{l=1}^k (\mathbf{O}_j \cdot \mathbf{e}_l) \mathbf{e}_l}{N_{\text{obs}}} \quad (4)$$

and \bar{O} . It is quite clear that about 50 eigenprofiles should be taken into account in order to recover, from a PCA analysis, a pseudo-line comparable to the SLA (i.e., \bar{O}) or LSD ones. This result is in clear contradiction with the comments made in §5.1 of Martínez González et al. (2008) about P_1 and LSD or SLA pseudo-profiles, using noisy but synthetic data. Indeed, PCA denoising can be made equivalent to the line addition technique, as well as to least-squares deconvolution, but for the TBLegacy data we have been using in that study, at the price of considering *a set of eigenprofiles* and *not* the only one associated with the largest eigenvalue of \mathbf{C} (and similar behaviours were noticed for II Peg and ε Eri data).

In order to understand this behaviour, it can be worthwhile analysing, in addition to the polarization data, the so-called “null” spectra, $N(\lambda)$, which comes along with standard Narval (and Espadons) data. It is indeed customary now in stellar spectropolarimetry to proceed with a *double beam-exchange* method

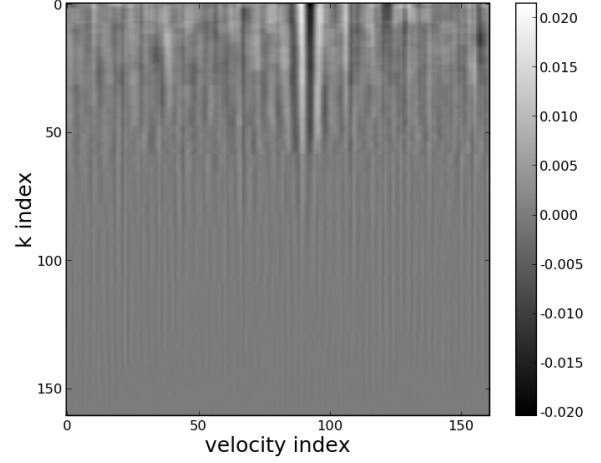


Fig. 5. Map of the $(P_k - \bar{O})$ from circular polarization observations of ε Eri made on February 2007. It takes about $k=50-60$ eigenprofiles for recovering the mean \bar{O} profile. The color scale on the right side of the image also indicates, in that case, that $P_{k=1}$ can be a factor of 2 smaller in amplitude than the SLA mean profile whose amplitude is about 0.04%.

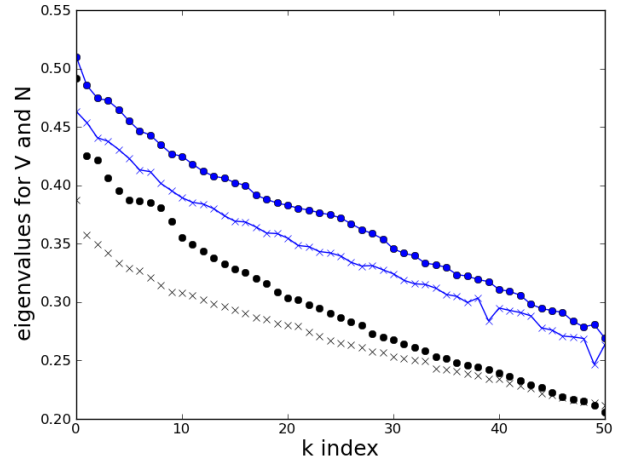


Fig. 6. Successive eigenvalues of the cross-correlation matrices computed respectively from the V (dotted lines) and the N (crossed lines) data of II Peg (discontinuous lines) and ε Eri (continuous lines) from TBLegacy. Eigenvalues for ε Eri were magnified by a factor of 10.

which consists in recording a sequence of 4 sub-exposures associated to 2 distinct and opposite polarization states (see e.g., Semel & Li 1996). N profiles result from a combination of sub-exposures, similar to the one used for the extraction of the polarization signal, but on the contrary *removing* any polarization signal of astrophysical origin. Its main usage is for the eventual detection of any spurious signal in the data which may corrupt the astrophysical signal. However, for clean observations (i.e., when $N(\lambda)$ is structureless), it basically contains noise, at the same level as the one which remains in the polarized spectra.

The number of eigenprofiles to consider for the reconstructed P_k to be comparable to LSD or SLA pseudo-profiles is roughly given by the index at which the sequences of eigenvalues of V and N , respectively, do overlap. Figure (6) displays two sets of

eigenvalues, which overlap indeed for $k \approx 50$ in these case. II Peg data is represented by discontinuous lines, while ε Eri data is represented by continuous lines (note also that for this latter set of data, eigenvalues were magnified by a factor of 10). In both case, V -eigenvalues correspond to dotted lines while cross symbols are for N -eigenvalues. The same kind of an empirical criteria was advanced by Martínez González et al. (2008) during their discussion about respective PCA analysis of a “correlated” (synthetic) data set and another one of uncorrelated (Gaussian) noise.

In summary, the *simultaneous* PCA analysis of V and N allow for (a) the *detection* of a polarized signature in the data, if the condition

$$s_i^{(V)} > s_i^{(N)} \quad (5)$$

is satisfied and (b) the *characterization* of a single representative signature, similar to LSD or SLA pseudo-profiles, which can be made considering projections of the original data on a number of eigenprofiles which will be given by this index at which the two sequences of eigenvalues $s_i^{(V)}$ and $s_i^{(N)}$ do overlap.

5. Intrinsic dimension of the dataset

We finally evaluate the intrinsic dimensionality of our main II Peg and ε Eri data sets, following the analysis exposed in Asensio Ramos et al. (2007) and illustrated with synthetic data and solar spectropolarimetric observations. To this end, we computed maximum likelihood dimension estimators \hat{m} for different values n of neighbours, for each of the profiles contained in the observations matrix \mathbf{O} .

We adopted the formula modified by MacKay & Ghahramani (2005)³ after the initial work of Levina & Bickel (2005). Both for II Peg and ε Eri data we have been analysing, values for \hat{m} appear in a range of the order of 38-48, for n ranging from 3 to 75. This is quite consistent with our PCA analysis of P_k vs. \bar{O} showing that our noisy data force us to consider more eigenprofiles than a priori expected, according to Martínez González et al. (2008).

6. Conclusion

We have experimented different methods of analysis of multiline polarized spectra of stars. We have shown, using real data, that the simple line addition technique (Semel et al. 2009) allows for the computation of pseudo-profiles very similar to the ones computed by least-squares deconvolution. It is also much simpler to implement and it requires less external input data, which makes it both simple and efficient, and therefore very suitable for the implementation of a standard post-processing tool for the TBLegacy database content.

From our study, LSD does not show any clear advantage on SLA. Furthermore, its systematic use for stellar spectropolarimetric databases would require, for the sake of interoperability, the set-up of a specific protocol concerning the line depth cut-off criteria and the normalization of weights used both for Stokes I and V data processing.

We have also applied PCA denoising to real (and noisy) observational data, which proves indeed very efficient. We have shown that it can provide an alternative to SLA or LSD post-processing methods, for the characterization of the polarization

content of the multiline observations, once the necessary number of eigenprofiles of the cross-product matrix of the observations have been carefully estimated. The latter can be derived from the combined PCA analysis of V and N data. Finally, and *as well as for SLA*, it is in principle equally *applicable to all kind of polarization signals*, whatever is their physical origin or the kind of observed state of polarization, circular or linear, which was observed.

Acknowledgements. This research has made use of the VizieR catalogue access tool, CDS, Strasbourg, France. The original description of the VizieR service was published in A&AS 143, 23. Narval data were provided by the Cnrs/Insu Bass2000-CDAB datacenter operated by the *Université Paul Sabatier, Toulouse-OMP* (Tarbes, France; <http://tblegacy.bagn.obs-mip.fr/>).

References

- Asensio Ramos, A., Socas-Navarro, H., López Ariste, A., Martínez González, M. J. 2007, ApJ, 660, 1690
- Berdugina, S. V., Jankov, S., Ilyin, I., Tuominen, I., Fekel, F. C. 1998, A&A, 334, 863
- Carroll, T. A., Kopf, M., Ilyin, I., Strassmeier, K. G. 2007, Astronomische Nachrichten, 328, 1043
- Donati, J.-F., Semel, M., Carter, B.D., Rees, D.E., Collier Cameron, A. 1997, MNRAS, 291, 658
- Donati, J.-F., Catala, C., Landstreet, J., Petit, P. 2006, Solar Polarization 4, ASP Conference Series, Vol. 358, Eds. Casini & Lites, 362
- Donati, J.-F., Gregory, S.G., Alencar, S.H.P., Bouvier, J., Hussain, G., Skelly, M., Dougados, C., Jardine, M.M., Ménard, F., Romanova, M.M., Unruh, Y.C. 2011, MNRAS, 417, 472
- Kochukhov, O., Makaganiuk, V., Piskunov, N. 2010, A&A, 524, 5
- Kochukhov, O., Makaganiuk, V., Piskunov, N., Snik, F., Jeffers, S. V., Johns-Krull, C. M., Keller, C. U., Rodenhuis, M.; Valenti, J. A. 2011, ApJ, 732, 19
- Koleva, M., Vazdekis, A. 2012, A&A, 538, A143
- Levina, E., Bickel, P.J. 2005, Advances in Neural Information Processing Systems, Vol. 17, Eds. Saul, Weiss & Bottou
- López Ariste, A., Casini, R. 2002, ApJ, 575, 529
- Martínez González, M. J., Asensio Ramos, A., Carroll, T. A., Kopf, M., Ramírez Vélez, J. C., Semel, M. 2008, A&A, 486, 637
- Piskunov, N. E., Kupka, F., Ryabchikova, T. A., Weiss, W. W., Jeffery, C. S. 1995, A&AS, 112, 525
- Ramírez Vélez, J. C., Semel, M., Stift, M., Martínez González, M. J., Petit, P., Dunstone, N. 2010, A&A, 512, 6
- Rees, D., Semel, M. 1979, A&A, 74, 1
- Rees, D., López Ariste, A., Thatcher, J., Semel, M. 2000, A&A, 355, 759
- Semel, M. 1989, A&A, 225, 456
- Semel, M. & Li, J. 1996, Sol. Phys., 164, 417
- Semel, M., Ramírez Vélez, J. C., Martínez González, M. J., Asensio Ramos, A., Stift, M. J., López Ariste, A., Leone, F. 2009, A&A, 504, 1003
- Skumanich, A., López Ariste, A. 2002, ApJ, 570, 379

³ <http://www.inference.phy.cam.ac.uk/mackay/dimension/> – see also Eq. (5) in Asensio Ramos et al. (2007)